Strain-Dependence of the Electronic Properties in Periodic Quadruple Helical G4-Wires

Rosa Di Felice,*,† Arrigo Calzolari,† Anna Garbesi,†,‡ Simone S. Alexandre,§ and José M. Soler§

National Center on nanoStructures and bioSystems at Surfaces (S3) of INFM-CNR, c/o Dipartimento di Fisica, Università di Modena e Reggio Emilia, Via Campi 213/A, 41100 Modena, Italy

Received: August 2, 2005; In Final Form: September 29, 2005

The electronic structure of periodic quadruple helix guanine wires, which mimic G4-DNA molecules, was studied as a function of the stacking distance between consecutive planes, by means of first principles density functional theory calculations. We show that, whereas for the native DNA interplane separation of 3.4 Å the HOMO- and LUMO-derived bands are poorly dispersive, the bandwidths can be significantly increased when compressive strain is applied along the helical axis. Our findings indicate that efficient band conduction for both holes and electrons can be supported by such wires for stacking distances below 2.6 Å, which imply a huge axial deformation with respect to double and quadruple helices in solutions and in crystals.

Introduction

G4-DNA is a quadruple helical structure of homoguanilic or guanine-rich sequences, that occur in a wide variety of natural situations and organisms. G4-DNA can be particularly important in the telomeric region of chromosomes, where it is responsible for edge protection against cell proliferation, with consequent envisaged applications in cancer treatment. It is also an excellent prototype case to study self-assembling at the supramolecular scale and the design of biomimetic systems. An excellent review of the chemicophysical and biological aspects of G4-DNA was recently published by Davis.[1]

On the other hand, G4-DNA molecules are currently attracting interest within the nanotechnology research community, in view of attaining conductive DNA-based wires for device fabrication.[2−4] This envisaged novel role of G4-DNA is proposed on the basis of some structural features, that are expected to influence the electronic characteristics in a device setup. (i) The peculiar in-plane arrangement of four guanines forming a tetrad, kept together by a double ring of eight hydrogen bonds (see Figure 1), endows the quadruple helices with a higher stiffness than the DNA double helices: this quality suggests an enhanced resistance against deformation fields to which the molecules are subjected when deposited onto substrates and/or attached to electrodes.[5] Consistent with this intuition, it is indeed observed by atomic force microscopy (AFM) and scanning tunneling microscopy (STM) imaging that G4-DNA has a higher persistence length than B-DNA.[6] (ii) The high molecular density in a cylindrical section with a diameter comparable to that of double helical DNA (2.3 nm versus 2.1 nm) induces also a more "continuous" charge density distribution and the consequent formation of channels for mobile charges through the bases along the stack.[7] (iii) The experimental evidence that the quadruplex arrangement is stabilized by the presence of metal cations in solution during the self-assembly step of the synthesis process[1,8] stimulates the idea that a metal wire is accommodated at the core of the molecule, which in principle could mediate charge motion, either by coupling to the bases or by intrinsic metallic behavior.[9] (iv) The rotation angle of 30° between adjacent guanines, smaller than in double stranded guanine-rich DNA sequences, might be an indication of a better $\pi-\pi$ overlap (that is expected to improve with decreasing angle[10]) influencing the performance as a π-way,[11] namely the ability to transport charges through the superposition of π orbitals along the stack.

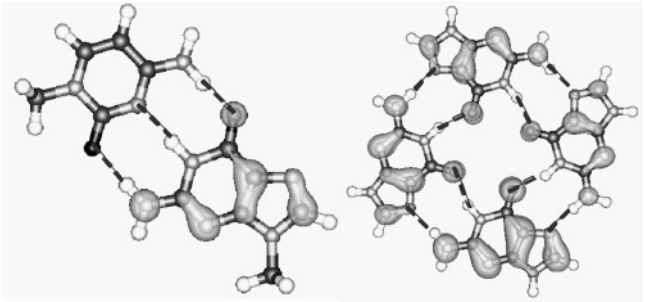

Figure 1. Structure and isosurface plot of the HOMO wave function for the GC pair of double helical DNA conformations (left) and for the G4 tetrad (right) that is the planar unit of the G4-wires. Spheres of increasing gray darkness stand for H, N, C, and O atoms. The dashed sticks identify the hydrogen bonds: there are eight hydrogen bonds per plane in G4-wires versus three (two) hydrogen bonds for GC (AT) pairs in double-stranded DNA.

Notwithstanding the above appealing features, it was recently shown[7] that theory does not predict a coherent band transport mechanism (a precondition for efficient current flow under applied voltage) for periodic G4-wires in which the stacking distance of 3.37 Å is that pertaining to crystallized short G4-DNA molecules.[8] However, following the recent characterization by AFM imaging of novel long G4-wires deposited on mica,[6] a possible axial contraction was proposed. Whether such strained structures exist and what their origin is (e.g., substrate lattice mismatch, details of the chemical synthesis, imaging perturbation) are open questions. In the meantime, stimulated by the intriguing suggestions, we performed a computational analysis

* Phone: +39-059-2055320. Fax: +39-059-2055651. E-mail: rosa@unimore.it.

† National Center on nanoStructures and bioSystems at Surfaces (S3) of INFM-CNR.

‡ CNR-ISOF, Area della Ricerca, Via P. Gobetti 101, 40129 Bologna, Italy.

§ Departamento de Física de la Materia Condensada, C.-III, Universidad Autónoma, 28049 Madrid, Spain.

10.1021/jp054274q CCC: $30.25
Published on Web 10/29/2005

to inquire about the consequences of the structural deformations on the electronic properties of infinite G4-wires, with a focus on understanding whether it is possible to induce a transition to a coherent band transport mechanism for a critical value of the axial strain. The effects of lattice strain on the electronic structure of inorganic crystals have been widely studied over the years, especially in the context of strained superlattices,[12] confinement in quantum dots,[13] and more recently ferroelectrics.[14] Here, we extend the analysis to new materials explored for nanotechnology and focus on physicochemical quantities that affect transport phenomena.

In the remainder of this article, we briefly describe the computational method and the simulated systems, then present the results and discuss their implications for the possible mechanisms of charge motion through G4-wires with relatively short interplane separation, and finally summarize our findings.

Computational Details

Our calculations were based on density functional theory (DFT) as implemented in the PWSCF code,[15] with the electron wave functions expanded in a basis set constituted of plane waves with kinetic energy up to 25 Ry and with the ion cores represented by non-norm-conserving pseudopotentials.[16] Gradient corrections in the PW91 parametrization were included in the exchange-correlation functional.[17] The periodic G4-wires were simulated by repeated supercells ($24.3 \times 24.3 \times 10.1\epsilon$) Å^3 wide (details in the Supporting Information), with ϵ being the parameter that measures the strain with respect to the crystal structure determined by Phillips and co-workers.[8] With our choice for the supercell, contiguous repeated wires are separated by a lateral vacuum thickness of about 16 Å, which is enough to consider them isolated, and, thus, the results apply to a single wire. The method was previoulsy tested on similar systems and on the individual components, the guanine molecules.[10,18] Taking for the strain parameter the definition $\epsilon = d/d_0$, with $d_0 = 3.37$ Å being the equilibrium stacking distance for the crystallized molecules and d being the strained stacking distance, we considered the following values: $\epsilon = 0.7418$ (−26%), 0.7715 (−23%), 0.8012 (−20%), 0.8309 (−17%), 0.9199 (−8%), 1.0089 (+1%), 1.0979 (+10%), and 1.1869 (+19%), corresponding to $d = 2.5$, 2.6, 2.7, 2.8, 3.1, 3.4, 3.7, and 4.0 Å. The backbone was excluded[19] for the strained structures, but we verified that its inclusion in the simulation of an unstrained wire does not yield any additional electronic levels in the energy range around the fundamental energy gap. Starting from the database X-ray structure for the short molecules of eight stacked planes,[8] we constructed an infinite periodic G4-wire with tetrameric planes separated by the equilibrium distance of 3.37 Å and fully relaxed its geometry[7] (the construction and periodicity unit are reported in the Supporting Information). Then, we changed the stacking distance to simulate axial strain, without further relaxing the atomic positions. The effect of atomic relaxation was qualitatively inspected only for the crucial intervalue separations of 2.6 and 3.4 Å, which pertain to a highly compressed and an unstrained wire, respectively. Since we are not focused here on metal−guanine coupling and we previously demonstrated that such a coupling with alkali cations is poor in the energy range close to the band gap,[7] we study in this report empty G4-wires, although such molecules are commonly stabilized by metal incorporation[18] and metals may determine the ultimate conduction capabilities.

The tests to determine the effect of the backbone and of the helical symmetry were performed only for the unstrained condition ($d = 3.4$ Å, twist = 30°) with the SIESTA code that allowed us to use a smaller atomic basis set while maintaining a reliable accuracy,[20,21] thus overcoming the computational burden. The technical parameters were equal to those employed in a previous investigation of double stranded DNA polymers.[22]

Results and Discussion

Axial Compression/Extension. In Figure 2, the band structure of the wires is reported for selected values of the strain ϵ, corresponding to a large compressive strain (top) and to a vanishing strain (bottom), to compare extreme situations. The nature of the band manifolds (12-plets) as due to the multiplicity of the guanine molecules in the simulation supercell was identified and explained in recent reports.[7,18] Note that the band structure was obtained by calculations that exploited only the translational symmetry of the wire, whereas the helical symmetry was not imposed: as a consequence, band grouping (each 12-plet should be divided into three sets of four bands) and degeneracies at Brillouin zone (BZ) edges are not respected.[3] Test calculations to verify that such symmetry principles are recovered if one imposes the helical symmetry to be strictly satisfied are discussed below. Some new features that appear under strain are noteworthy: (i) the band gap decreases from 3.02 to 2.27 eV upon axial compression of 23%;[23] (ii) whereas in the unstrained wire the top manifold of energy bands is separated by a large gap (0.7 eV) from the underlying manifolds, in the highly strained wire such a gap is strongly suppressed and becomes almost vanishing (0.2 eV), thus originating a wide *effective* "continuum"; and (iii) the dispersion[24] of each individual band, as well as the amplitude of the manifolds, is increased under strain. We elaborate more deeply on these issues in the following, by identifying a few key quantities and analyzing their behavior as a function of the stacking distance.

To understand the strain dependence of the electronic structure, we focus on the following data: the amplitude of the HOMO manifold, labeled as Δ_{HOMO}; the fundamental band gap between the occupied and empty electron states, labeled as E_{g0}; the total amplitude of the four highest energy occupied manifolds, labeled as Δ_{HO4}; the energy gap, labeled as E_{g1}, between the lower edge of the HOMO manifold and the upper edge of the manifold immediately below it in the energy scale; and the bandwidth of the highest occupied (lowest unoccupied) band in the HOMO (LUMO) manifold, labeled as δ_{HOMO} (δ_{LUMO}). A negative (positive) value of δ_{HOMO} (δ_{LUMO}) indicates a downward (upward) bending of the band from the center to the edge of the one-dimensional BZ. The Δ and E_{gn} parameters are schematically defined in Figure 3. In Figure 4, the thus defined parameters are reported as a function of strain. Our results indicate a tendency to saturation, roughly above a stacking distance of 2.8 Å (17% compressive strain), for all the examined quantities except for δ_{LUMO}. The degree of saturation is not so perfect for all the quantities. Let us first discuss the HOMO bandwidth, δ_{HOMO}, for which this saturating behavior is indeed clear: δ_{HOMO} is a measure of the extent to which the axial $\pi-\pi$ interaction is really able to induce a coherent bandlike mechanism for charge mobility. The larger δ_{HOMO} and the smaller the separation from the other occupied bands, the closer the material resembles a bandlike bulk (semi-) conductor, with a continuum of energy levels where free charge carriers either exist intrinsically or may be introduced by suitable doping mechanisms. The plot in Figure 4e indicates that, although G4-wires in normal conditions (zero strain) are characterized by a poor HOMO bandwidth (10−20 meV, upward dispersion), this feature may be enhanced under compression. However, only for a high strain of 26% does it become as high as 160 meV in

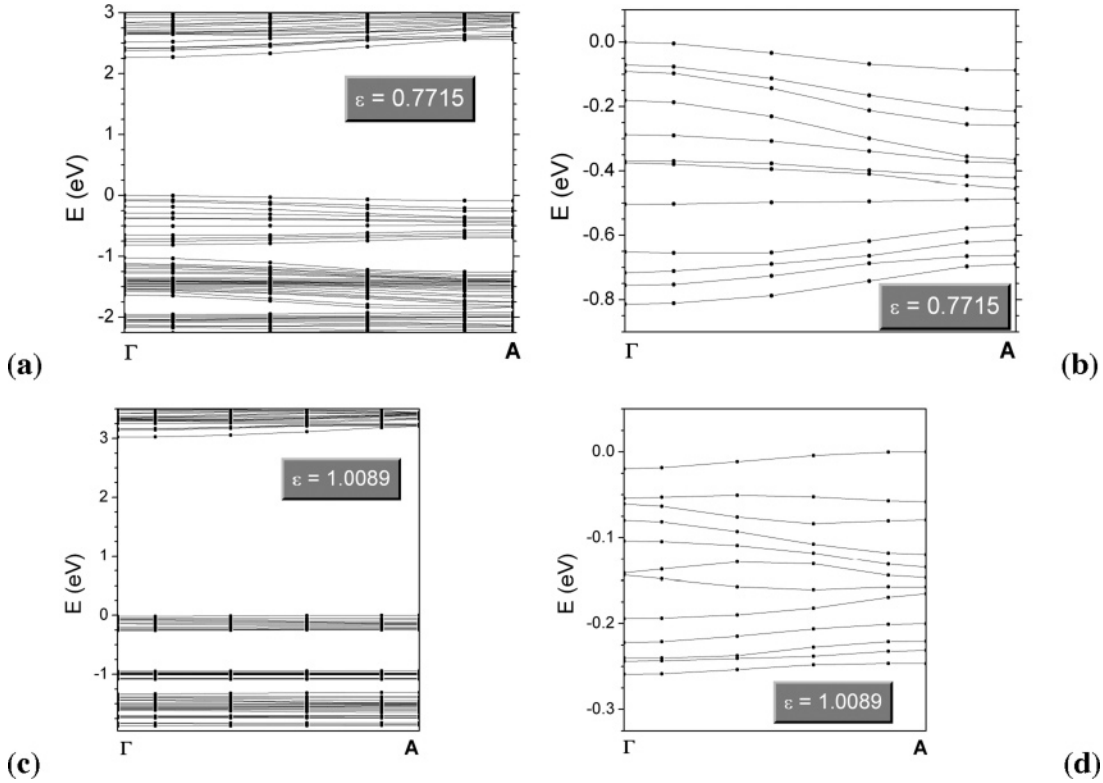

Figure 2. Band structure in the energy range around the band gap (left) and a close-up of the HOMO manifold (right) for two selected values of the strain, indicative of a highly strained wire (a and b) compressed by 23% with a stacking distance equal to 2.6 Å and of an almost unstrained wire (c and d) with a stacking distance equal to 3.4 Å. The horizontal axis reports values of the Bloch wave vector along the axial Brillouin zone (BZ) parallel to the axis of the quadruple helix: Γ and A are the center and the edge of the BZ, respectively. The origin of the energy scale is set at the highest occupied eigenvalue for each wire. In c and d, the vertical scale is chosen to include in the occupied portion (negative energy values) an equal number of band manifolds, i.e., 4. The band structure is reported here for the unrelaxed configurations, obtained by just changing the interplanar distance with respect to the equilibrium G4-wire with $d = 3.37$ Å.

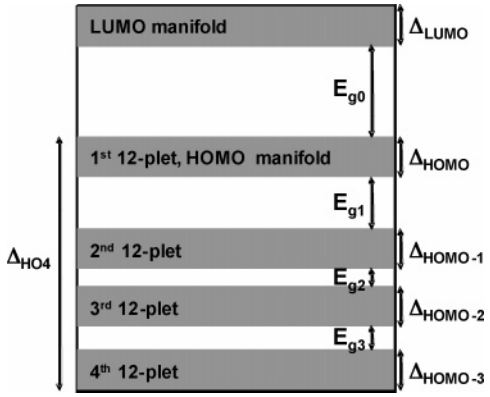

Figure 3. Definition of the band structure parameters that are used to analyze the strain dependence. $\Delta_{HOMO} = \max_{\Gamma A}(\text{HOMO manifold}) - \min_{\Gamma A}(\text{HOMO manifold})$; all the other Δ's are defined accordingly. $E_{g0} = \min_{\Gamma A}(\text{LUMO manifold}) - \max_{\Gamma A}(\text{HOMO manifold})$. These quantities are defined to follow the effect of compression on the energy spread of guanine levels in the quadruple helix; the Brillouin zone resolution is not important to this purpose.

absolute value (downward dispersion), whereas, for a 23% strain, which is still very high, δ_{HOMO} is immediately depressed to 80 meV (maintaining the downward dispersion). This trend, at a first sight, suggests that it would be rather unlikely to exploit axial compression to induce a *real* bandlike behavior for the G4-wires. However, a closer look at the computed data reveals other relevant effects. In particular, Figure 4e shows a clear transition from an upward to a downward dispersion, from the origin to the edge of the Brillouin zone, for a compressive strain larger than 13%. We remark that downward dispersion is typical of inorganic semiconductors, whose effective mass is determined by the curvature of the highest occupied band around the *k* point in the BZ where the maximum occurs.

In addition to the above comments, a more thorough inspection of Figure 4 reveals that the $|\delta_{HOMO}|$ increase upon axial compression goes along with the increase of Δ_{HOMO} and Δ_{HO4} and the decrease of E_{g0} and E_{g1} (Figure 4a−d). Whereas we do not wish to speculate here about how the changes in the fundamental band gap (E_{g0}) may be interpreted and exploited, we point out the meaning of the trends in the occupied portion of the band structure, focusing on Δ_{HOMO} and E_{g1}. It was recently discussed[7] that the electronic properties of the guanine quadruplexes are characterized by *effective* bands whose *effective* bandwidth is given by the amplitude of the HOMO-derived 12-plet, i.e., Δ_{HOMO}. Consistent with this interpretation, it is immediately clear that when this quantity increases (for small stacking distances), the motion of charge carriers is enhanced, because there is good wave function coupling[25] over a broad energy range. The analysis presented here reveals in particular that for $d = 2.6$ Å coherent charge motion is characterized by a δ_{HOMO} of 80 meV, but it is also assisted by incoherent mechanisms for an *effective* band amplitude of 800 meV.[26] Not only that, it is clear from Figure 4d that, whereas for the unstrained G4-wire the HOMO manifold (12-plet) is separated from the underlying one by an energy gap of 0.7 eV, this gap is strongly reduced to 0.2 eV for a 23% axial compression and totally vanished for a 26% axial strain. This observation implies that the total number of bands available for charge mobility (though partially incoherent) is not limited to the 12 bands in the top manifold but is widened to also include the underlying manifolds, as the value of E_{g1} is more and more reduced and

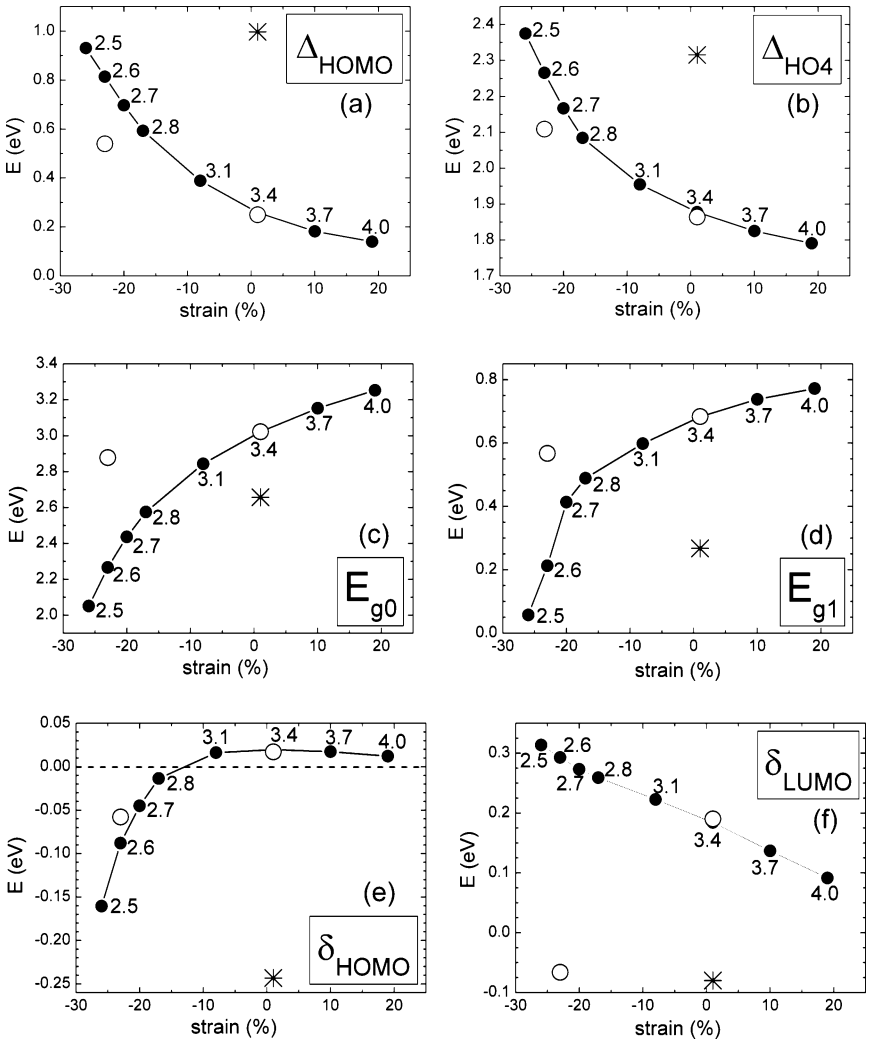

Figure 4. Strain dependence of some key band structure parameters, as defined in the text. The strain is reported on the horizonal axis as a percentage value of the quantity $(d - d_0)/d_0$, and the corresponding stacking distance d used in the calculations is explicitly written in each panel beside each computed dot. The lines just connect the computed data and do not correspond to any fit. Negative (positive) values on the horizontal axis pertain to axial compressive (tensile) strain. Dots (circles) represent results obtained without (with) atomic relaxation for the G4-wires with a three-plane periodicity unit. Asterisks are results relative to an uncompress G4-wire ($d = 3.4$ Å) with eclipsed planes. (a) The total amplitude (absolute value) of the highest occupied 12-plet of bands. (b) The total amplitude (absolute value) of the four topmost 12-plets, containing 48 bands. (c) The fundamental band gap $\min\{E_{\mathrm{LUMO}}\} - \max\{E_{\mathrm{HOMO}}\}$, where the minimum and the maximum values are taken over the LUMO and HOMO 12-plets, respectively, accounting also for the dispersion across the BZ. (d) The first band gap in the occupied manifolds, $\min\{E_{\mathrm{HOMO}}\} - \max\{E_{\mathrm{HOMO-1}}\}$. (e) The bandwidth of the highest occupied energy band in the HOMO 12-plet (negative (positive) values indicate downward (upward) dispersion, and the horizontal dashed line is a guide to the eye to mark the dispersion inversion). (f) The bandwidth of the lowest unoccupied energy band in the LUMO 12-plet (always positive, meaning upward dispersion).

finally annihilated.[27] From a closer inspection of the top four 12-plets, it appears that for $d = 2.6$ and 2.5 Å, they cover a practically continuous energy range of 2.3−2.4 eV. Once again, it is important to note that this range is not really covered by a *true* continuum of bands but rather by an *effective* continuum of bands with a poor intrinsic dispersion but separated from each other by very small amounts (a few tens of eV's) that facilitate an easy coupling at different energy values. This coupling is allowed by the existence of a high charge density in a limited spatial range, that may be understood by plotting the squared wave functions.[7]

The analysis of the electronic properties of the strained G4-wires is completed in Table 1 by a systematic report of all the relevant parameters, those plotted in Figure 4 and some others defined in the table footnote and in Figure 3. We just note that the fact that E_{g1}, E_{g2}, and E_{g3} are simultaneously vanishing for a stress of −26% reflects the attainment of a unique broad *effective* band with an amplitude of 2.38 eV.

Nonaxial Structural Changes. We qualitatively inspected the robustness of the above trends against other structural deformations that would accompany the axial compression/extension. In particular, for the periodic G4-wires with stacking distances of 2.6 and 3.4 Å, we allowed for atomic relaxation to minimize the forces. The results are indicated by the open circles in Figure 4. The structure with $d = 3.4$ Å was practically already at equilibrium (the 30° twist between any two planes does not change); hence, no significant difference between the dots and the open circles can be pointed out in Figure 4. Instead, the wire with $d = 2.6$ Å undergoes strong distortions upon atomic relaxation: the forces remain large, indicating that this configuration is not compatible with the periodicity constraint imposed with the unit supercell that contains three planes. In fact, we note that consecutive planes have a tendency toward enhanced twisting (thus breaking the modulo-3-plane symmetry), possibly to counteract the $\pi-\pi$ repulsion that becomes dominant at very small stacking distances. Although the open circles relative to

TABLE 1: Electronic Structure Parameters for the Strained G4-Wires[a]

strain (%)	Δ_{HOMO}	Δ_{HOMO-1}	Δ_{HOMO-2}	Δ_{HOMO-3}	E_{g0}	E_{g1}	E_{g2}	E_{g3}
−26	0.93	0.61	0.46	0.37	2.05	0.06	−0.08	0.02
−23	0.81	0.44	0.45	0.34	2.27	0.21	−0.05	0.05
−20	0.70	0.26	0.44	0.33	2.44	0.41	−0.03	0.06
−17	0.59	0.21	0.44	0.31	2.58	0.49	0.00	0.04
−8	0.39	0.16	0.32	0.30	2.84	0.60	0.17	0.02
+1	0.26	0.14	0.27	0.28	3.02	0.68	0.23	0.02
+10	0.18	0.13	0.22	0.27	3.15	0.74	0.26	0.01
+19	0.14	0.13	0.20	0.27	3.25	0.77	0.28	0.00

[a] Δ_{HOMO-1}, Δ_{HOMO-2}, and Δ_{HOMO-3} are the amplitudes of the first, second, and third band manifolds, respectively, each constituted of 12 bands, below the HOMO. E_{g2} and E_{g3} have a meaning similar to E_{g1}: they separate the occupied manifolds from each other (E_{g2} is for the second from the third 12-plet, and E_{g3} is for the third from the fourth 12-plet).

−23% strain in Figure 4 must be interpreted with care, because they do not correspond to a metastable geometry, they qualitatively indicate an alteration of the very smooth and saturating trends identified by the dots. However, as an additional test, we computed the bandstructure of a 23% compressed periodic wire ($d = 2.6$ Å) characterized by an interplane twist of 45° (2-plane periodic supercell), to verify whether high twist angles necessarily imply a reduction of the bandwidths δ_{HOMO} and Δ_{HOMO}. The results (Supporting Information) indicate that this is not the case: indeed, for such a strained wire with respected periodicity, the bandwidths are notably increased with respect to those marked by the dots in Figure 4. Therefore, our results indicate that large bandwidths and small band gaps are indeed attainable for G4-wires with a short interplane separation. In addition, the asterisks in Figure 4, relative to an eclipsed G4-wire with $d = 3.4$ Å, show that large bandwidths and small band gaps are also attainable with other kinds of structural deformations, such as a change of the twist angle, even for unstrained wires.[10]

Let us, finally, briefly comment on the possible implications of the present results. AFM images of long G4-wires reveal that these molecules may be advantageous for nanotechnology applications, with respect to the parent poly(dG)−poly(dC) polymers employed for the chemical synthesis,[6,28] because of higher stiffness and stability and the good resistance of the structural features when deposited onto an inorganic substrate. Our analysis predicts that, if the stacking distance between consecutive planes along the quadruple helices were dramatically shortened with concomitant, precise control of the accompanying deformations, this structural compression could be effective in improving the electrical behavior, making these helices appealing molecular nanowires.

Effect of the Helical Symmetry on the Computed Bands. Artacho and co-workers[29] recently showed that, for an A-DNA molecule with a uniform poly(G)−poly(C) sequence, the energy levels obtained at the Γ point of the Brillouin zone (BZ) of the 11-plane unit cell may be unfolded into 11 *k* points in the BZ of a corresponding 1-plane perfectly helical unit cell. Figure 1 of their paper plots the bands against the wave-vector spanning the large 1-plane BZ, valid only under the constraint of helical symmetry. If one plots the same bands in the 11-plane BZ, each band would be a multiplet of 11 bands (11-plet), with degeneracies at the BZ center and edge, as long as the helix is perfect: the degeneracies are broken if the helical degree of freedom is relaxed. Such an unfolding is useful because few DFT codes are prepared to exploit helical symmetry, and they require the use of supercells with translational symmetries.

In principle, the unfolding can be performed for the full bandstructure. However, in practice, the use of plane waves or real-space grids with specific orientations, as well as the small interactions between the artificially repeated unit cells in the directions perpendicular to the axis, produce slight breakings of the helical symmetry, which may be amplified during structural relaxation. In addition, in our case, the initial geometries were taken from X-ray experiments of finite G4 fragments, which do not necessarily have a perfect helical order because of an inherent structural flexibility characteristic of molecules with respect to crystals: this realistic symmetry relaxation is the reason that the perfect band unfolding is not observed in Figure 2.

For a symmetric G4 plane, we expect that each guanine molecular state gives rise, through the small hydrogen-bond interactions, to a quadruplet of states with the following symmetries: + + + +, + + − −, + − + −, and + − − +. In a periodic helix, each of these states will give rise to one band, which will appear folded three times in the BZ of a 3-plane supercell, resulting in the observed 12-plets. Indeed, we show here for an unstrained G4-wire in Figure 5b that, if the helical symmetry is imposed, the bands in the HOMO 12-plet have the expected symmetries. Without entering into the details of the band characters that would allow us to unfold them into the corresponding helical 1-plane BZ, we just point out that this comparison reconciles our results with the interpretation of band dispersion in helical DNA-based periodic wires.[29]

The differences with the bands obtained by releasing the constraint of helicity are rather minor: some bands become degenerate, and in general, they become flatter and narrower. The main difference is a strong flattening of the HOMO 12-plet, that in the symmetric case is ∼0.08 eV wide instead of 0.3 eV for the nonsymmetric case, and a decrease of the E_{g1} value (the gap between HOMO and HOMO-1 12-plets, see text), which becomes 0.3 eV instead of 0.7 eV. It is difficult to assess which quantitative details are best representative of reality: on one hand, the configuration represented in Figure 2 can be considered to be just a snapshot of the dynamic reality; on the other hand, the situation represented in Figure 5 is a sort of average symmetrization which bypasses particular snapshots, but the exact symmetry may be an unrealistic artifact.

Bandstructure Features due to the Backbone. To prove the relevance of the bandstructure obtained for the model G4-wires made only of the base stack, on which basis we discussed above the effect of structural deformations, we did calculations for similar wires including the sugar−phosphate backbone, while still neglecting the counterions and saturating the lateral dangling bonds by H atoms. These tests were performed only for the unstrained condition ($d = 3.4$ Å, twist = 30°) with the SIESTA code[20,21] and previously optimized technical details.[22] The results plotted in Figure 5c and d demonstrate that the backbone does not significantly influence the values of Δ_{HOMO}, δ_{HOMO}, and E_{g0}, which mostly influence the ease of charge motion. This finding is in line with a recent Car−Parrinello simulation of Z-DNA,[30] whose results revealed that only the counterions, and

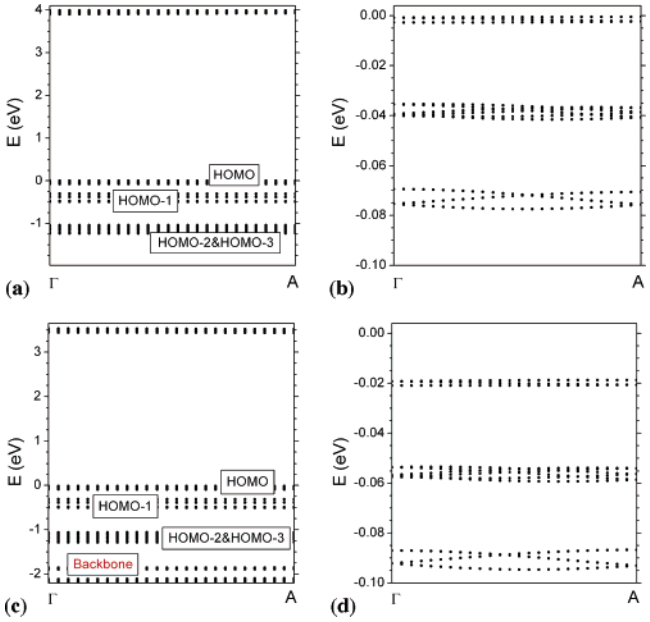

Figure 5. (top) Band structure of a periodic G4-wire computed in a three-plane unit cell, with a 3.4 Å stacking distance and without the backbone, constructed by imposing the full symmetry of the periodic G4 helix to the average geometry of the relaxed structure (including the backbone) and removing the backbone atoms: (a) energy range around the fundamental band gap; (b) detail of the HOMO 12-plet (this, particularly on a smaller energy scale, reveals the band grouping and the expected degeneracies at the BZ edges). (bottom) Band structure of a G4-wire for the same geometry as in the top panels but including the backbone atoms: (c) energy range around the fundamental band gap (a new 12-plet formed by electron states localized on the phosphates appears at ∼2 eV below the HOMO); (d) detail of the HOMO 12-plet (only a slight downward shift by ∼20 meV is detected with respect to the case without the backbone (part b). The band structure description in terms of manifolds remains valid also when including the backbone, thus not affecting the results about the axial-strain dependence of the band structure parameters. These calculations were done with the SIESTA code.[20,21,22]

not the backbone, yield new electronic levels in the fundamental band gap. A new 12-plet of phosphate states appears at ∼2 eV below the HOMO, leaving the band multiplets in the energy range above it practically unchanged. This finding supports the analysis of deformation effects done on the basis of results obtained without the backbone.

Summary

We investigated the bandstructure of G4-wires by means of ab initio DFT calculations. We examined issues that are appealing for implications in nanotechnology (the effects of axial and rotational strains), as well as inherent computational issues (the roles of symmetries and the backbone).

We showed that the bandstructure parameters can be tuned by structural factors. In particular, both axial compression and twist variation are able to enhance the $\pi-\pi$ overlap and to increase the bandwidth values. However, the critical strains for which significant changes become promising for molecular electronics applications are rather large and would likely be hampered under normal laboratory conditions. Notwithstanding this limitation, the trends for the structure/electronic-structure relationship identified in our work maintain a remarkable value: they underline fundamental physicochemical effects and their extension from inorganic crystals to one-dimensional polymers, and they may, in principle, trace the route to plan/realize an alternation of segments with different electrical responses along a G4-wire and to interpret electrical measurements if experiments on such systems progress.[6,28]

We verified that the neglect of the backbone does not compromise these results and that the release of the helical symmetry is responsible for the failure of band unfolding.

Acknowledgment. Danny Porath is acknowledged for stimulating discussions and critical reading of the manuscript. This work was supported by the EC through Contract IST-2001-38951. R.D.F., A.C., and A.G. acknowledge the financial aid of the INFM Parallel Computing Initiative for the allocation of computer time on the supercomputers at CINECA (Bologna) and of MIUR-IT through Project FIRB-NOMADE and the continuous scientific support of Elisa Molinari. S.S.A. and J.M.S. acknowledge fruitful discussions with Emilio Artacho and Grant BFM2003-03372 from the Spain Ministry of Science.

Supporting Information Available: Figures S1 and S2 depicting the construction of the periodic G4-wires from finite crystallized G4-DNA molecules and the effect on the band structure of structural distortions induced by altering the twist angle of the G4-wires, respectively. This material is available free of charge via the Internet at http://pubs.acs.org.

Note Added after ASAP Publication. This paper was posted ASAP on October 29, 2005. A correction was made to an author's name. The paper was reposted on November 1, 2005.

References and Notes

(1) Davis, J. T. *Angew. Chem., Int. Ed.* **2004**, *43*, 668−698.
(2) Endres, R. G.; Cox, D. L.; Singh, R. R. P. *Rev. Mod. Phys.* **2004**, *76*, 195−214.
(3) Porath, D.; Cuniberti, G.; Di Felice, R. *Top. Curr. Chem.* **2004**, *237*, 183−227.
(4) Di Ventra, M.; Zwolak, M. DNA Electronics. In *Encyclopedia of Nanoscience and Nanotechnology*; Nalwa, S. H., Ed.; American Scientific Publishers: Stevenson Ranch, CA, 2003.
(5) Muir, T.; Morales, E.; Root, J.; Kumar, I.; Garcia, B.; Vellandi, C.; Marsh, T.; Henderson, E.; Vesenka, J. *J. Vac. Sci. Technol., A* **1998**, *16*, 1172−1177.
(6) Kotlyar, A. B.; Borovok, N.; Mototsky, T.; Cohen, H.; Shapir, E.; Porath, D. *Adv. Mater.* **2005**, 1901−1905.
(7) Calzolari, A.; Di Felice, R.; Molinari, E.; Garbesi, A. *J. Phys. Chem. B* **2004**, *108*, 2509−2515; correction, *J. Phys. Chem. B* **2004**, *108*, 13058.
(8) Phillips, K.; Dauter, Z.; Murchie, A. I. H.; Lilley, D. M. J.; Luisi, B. *J. Mol. Biol.* **1997**, *273*, 171−182. X-ray structure ID UDF062.
(9) Di Felice, R.; Calzolari, A.; Zhang, H. *Nanotechnology* **2004**, *15*, 1256−1263.
(10) Di Felice, R.; Calzolari, A.; Molinari, E.; Garbesi, A. *Phys. Rev. B* **2002**, *65*, 045104.
(11) Eley, D. D.; Spivey D. I. *Trans. Faraday Soc.* **1962**, *58*, 411.
(12) Stroppa, A.; Peressi, M. *Phys. Rev. B* **2005**, *71*, 205303.
(13) He, L.; Bester, G.; Zunger, A. *Phys. Rev. B* **2005**, *72*, 081311.
(14) Bungaro, C.; Rabe, K. M. *Phys. Rev. B* **2004**, *69*, 184101.
(15) Baroni, S.; Dal Corso, A.; de Gironcoli, S.; Giannozzi, P. http://www.pwscf.org.
(16) Vanderbilt, D. *Phys. Rev. B* **1990**, *41*, 7892−7895.
(17) Perdew, J. P.; Chevary, J. A.; Vosko, S. H.; Jackson, K. A.; Pederson, M. R.; Singh, D. J.; Fiolhais, C. *Phys. Rev. B* **1992**, *46*, 6671−6687.
(18) Calzolari, A.; Di Felice, R.; Molinari, E.; Garbesi, A. *Appl. Phys. Lett.* **2002**, *80*, 3331−3333.
(19) Electron transfer through the helix is most likely due to the intrinsic electronic structure of the base stack. Note, however, that guanine quadruplexes are formed both with a DNA-like backbone of sugar rings and phosphates and without it. In the latter case, the guanines are usually decorated by lateral alkyl chains. See, e.g., ref 1 and: Gottarelli, G.; Spada, G. P.; Garbesi, A. In *Comprehensive Supramolecular Chemistry*; Atwood, J. L., Davies, J. E. D., MacNicol, D. D., Vögtle, F., Eds.; Pergamon: Elmsford, NY, 1996; Vol. 9.
(20) Ordejón, P.; Artacho, E.; Soler, J. M. *Phys, Rev. B* **1996**, *53*, R10441−R10444.
(21) Soler, J. M.; Artacho, E.; Gale, J. D.; García, A.; Junquera, J.; Ordejón, P.; Sánchez-Portal, D. *J. Phys.: Condens. Matter* **2002**, *14*, 2745−2779.

(22) Alexandre, S. S.; Artacho, E.; Soler, J. M.; Chacham, H. *Phys. Rev. Lett.* **2003**, *91*, 108105.

(23) Note that these are values computed within DFT. They are affected by an underestimate which may be as large as 50% of the real band gap and are, hence, unreliable for a quantitative *absolute* analysis. However, they may be used for a *comparative* analysis to understand the trends induced by the application of strain to the wires.

(24) The band dispersion is the dependence of the energy, for a given energy level, on the wave vector associated with the axial direction: this quantity contains the details of the shape of a band. The bandwidth is instead the total amplitude of a given band, e.g., the difference between the maximum and the minimum energy values in the band.

(25) This is the electronic factor in Marcus' electron-transfer theory. Marcus, R. A.; Sutin, N. *Biochim. Biophys. Acta* **1985**, *811*, 265. Voityuk, A. A.; Rösch, N.; Bixon, M.; Jortner, J. *J. Phys. Chem. B* **2000**, *104*, 9740−9745.

(26) The increase of the HOMO-manifold bandwidth upon reducing the interplane separation in G4-wires is consistent with the increase of transfer integrals in stacked GC pairs under similar compression conditions reported earlier by: Voityuk, A. A.; Rösch, N.; Bixon, M.; Jortner, J. *J. Phys. Chem. B* **2000**, *104*, 9740−9745.

(27) We point out that interplane wave function coupling is not so effective between different 12-plets as in the same 12-plet, because of the different charge distributions of the guanine orbitals in the HOMO, HOMO-1, etc.

(28) Kotlyar, A. B.; Borovok, N.; Molotsky, T.; Fadeev, L.; Gozin, M. *Nucleic Acids Res.* **2005**, *33*, 525−535.

(29) Artacho, E.; Machado, M.; Sánchez-Portal, D.; Ordejón, P.; Soler, J. M. *Mol. Phys.* **2003**, *101*, 1587−1594.

(30) Gervasio, F. L.; Carloni, P.; Parrinello, M. *Phys. Rev. Lett.* **2002**, *89*, 108102.